Nanomed Res J 5(4):369-377, Autumn 2020

RESEARCH ARTICLE

Bio efficacy, and photocatalytic activity of the silver nanoparticles synthesized from *Cryptolepis buchanani* leaf extract

Sudipta Panja [1], Anutosh Patra [1], Kalyani Khanra [1], Indranil Choudhuri [1], Bikas Ranjan Pati [2], Nandan Bhattacharyya [1,*]

[1] Department of Biotechnology, Panskura Banamali College, P.O. – Panskura R.S., Purba Medinipur, West Bengal, PIN- 721152, India

[2] Department of Microbiology, Vidyasagar University, Medinipur, West Bengal, PIN - 721102, India

ARTICLE INFO

Article History:
Received 18 Aug 2020
Accepted 22 Oct 2020
Published 01 Nov 2020

Keywords:
Cryptolepis buchanani
Silver nanoparticle
Green synthesis
Cytotoxicity
Photocatalytic activity

ABSTRACT

The aim of this study is to synthesize silver nanoparticles from the leaf extract of *Cryptolepis buchanani,* a medically important plant, by green synthesis method and determine it's bio-efficacy and photocatalytic activity study. The synthesized nanoparticles have an average size of 17.05±5.27 nm, crystalline in nature with face cantered cubic structure, and positive surface charge. The nanoparticles are biologically active. It killed > 90 % of HeLa cells at 25 µg mL^{-1} concentration *in-vitro* cell cytotoxicity assay, with a LD_{50} value of 3.98 µg mL^{-1}. The nanoparticles are less effective on MCF-7 and HEK-293 cell line, almost 70 % of MCF-7 populations were survived at highest concentration of 25 µg mL^{-1}. In case of HEK-293 it killed almost 78 % of cells at the same concentration with a 9.45 µg mL^{-1} LD_{50} value. The synthesized nanoparticle lysed less than 2.5 % of red blood cells at 10 µg mL^{-1} concentration *in-vitro*. The nanoparticles degraded >90 % of methylene blue dye in presence of light in 8.5 h. These properties of the synthesized nanoparticles are unique, and make it promising for its future potential applications.

How to cite this article
Panja S, Patra A, Khanra K, Choudhuri I, Ranjan Pati B, Bhattacharyya N. Bio efficacy, and photocatalytic activity of the silver nanoparticles synthesized from Cryptolepis buchanani leaf extract. Nanomed Res J, 2020; 5(4): 369-377. DOI: 10.22034/nmrj.2020.04.009

INTRODUCTION

Cryptolepis buchanani, is a medically important plant belonging to the Apocynaceae family. *C. buchanani* is commonly habitant in hot, deciduous forests and distributed throughout India [1]. The plant is used traditionally as medicine in loss of appetite, fever, skin diseases, curing bone fracture, diarrhea, and cough. It is considered as anti-inflammatory, antibacterial, blood purifier, and prescribed to children for rickets [2-5]. The plant *C. buchani*is full of various phytochemicals like nicotinoyl glucoside [6], buchanin[7], sarvero-genin, isosarverogenin glycosides[8], cryptosin[9], cryptolepain[10].

Previous studies explored some interesting properties of *C. buchani* plants. Ethanolic extract of stem has anti-inflammatory potential [11], root extract has immunopotentiating properties [5], plant extract has analgesic, anti-inflammatory, and chondroprotective activities [12], antioxidant and hepatoprotective activity [13], insecticidal activity [14], anti-dermatophyte activity [15].

Enrichment of phytochemicals in *C. buchanani* plant extract seeking attention for its alternative application. Recent study showed that gold nanoparticles from *C. buchanani* antimicrobial and catalytic Properties [16]. Plant materials are widely used for green synthesis of nanoparticles [17-22] as organic compounds act as capping and reducing agents. Green synthesis of nanoparticles is inexpensive, eco-friendly, and preferable than the traditional physical or chemical process [23]. Nanoparticles have a large surface to volume ratio, resulting from their very small sizes, making them more active than the bulk materials. Due to

* Corresponding Author Email:
bhattacharyya_nandan@rediffmail.com

their enhanced physicochemical properties and biological activities in comparison with the bulk materials, nanoparticles are effectively used in a wide range of areas, like medicine, engineering, catalysis, and environmental remediation [24,25]. In this study silver nanoparticles were prepared from *C. buchanani* leaves extract, characterized, and evaluated its biological and photocatalytic activity.

MATERIALS AND METHODS

Materials

The Plant materials (leaves of *Cryptolepis buchanani*) were collected from *Amlachati*, Pashchim Medinipur, West Bengal, India (22˚22′36″ N, 87˚02'36" E) during the season of summer season. The plant was identified by the experts of the "*Ex-situ* conservation site of Medicinal plant species" (*Amlachati*, West Bengal, India). The voucher specimen (herbarium code:PBC/15-16/Phd-109) was archived at the Department of Botany, Panskura Banamali college.

Synthesis of silver nanoparticles

The nanoparticles from plant leaves were synthesized by the green synthesis method described earlier [26] with modifications. The plant materials were cleaned thoroughly with running water for 15 minutes, followed by distilled water for 5 minutes, and allowed to dry in air. 10 g of the dry chopped leaves were homogenized with 100 mL of deionized water and boiled at 80 °C in a water bathfor 1 h to prepare leaf extract. The extract was filtered through 0.6 µm filter papers. One mM $AgNO_3$ and aqueous leaf extracts was mixed in 1:9 v/v ratio and incubated at 90 ^{0}C for 1 hour. Changing of color from light to deep brown during the reaction confirmed synthesis of the silver nanoparticles (AgNP) [27]. After reaction, the synthesized AgNPs were separated from colloidal suspension by centrifugation, and washed as described earlier. [27,28]. Finally, the pellet was dried to obtain the AgNPs.

Unlike other methods, this method neither required any hazardous chemicals like hydrazine, sodium borohydride, etc., nor to maintain any physical and chemical parameters like temperature, pressure, or pH. In this approach, the phytochemicals and other organic compounds present in plant extract were reduced the Ag^+ ions, and act as a stabilizing agent. In contrast, highly toxic chemicals used in chemically synthesis processes may be absorbed on the surface of nanoparticles, which might be toxic to health and the environment. These advantages make the single-step green synthesis process is inexpensive, less toxic, less harmful, and eco-friendly process.

Characterization of silver nanoparticles

UV-Vis spectrum was recorded from 300 nm to 800 nm with a resolution 1 nm [27, 29] by using UV-Vis spectrophotometer (Eppendorf BioSpectrometer). The shape and particle size and shape of the synthesized AgNPs was studied by Transmission electron microscopy (TEM) [23]. In this study, JEM-1200EX electron microscope (JEOL, Tokyo, Japan) was used and operated at an accelerating voltage of 120 kV. Particle sizes were analyzed by Image J v 1.53a software. The size distribution and potential stability in colloidal suspension of the synthesized AgNPs were studied by Dynamic light scattering (DLS) and Zeta potential respectively [30, 31]. Fourier transform infrared spectroscopy [31] (FTIR) spectrum was recorded by the Perkin-Elmer spectrometer FTIR Spectrum Two within the range of 4000 to 400 cm^{-1} with a resolution of 1 cm^{-1}. X-ray diffraction (XRD) analysis was conducted by X'pert-pro X-ray diffractometer at a voltage of 40 kV. Current of 30 mA in 2θ angle pattern. Cu K, radiation is used to record the spectrum in the range of 20° to 100° [31-32].

Cytotoxicity study

HeLa, MCF7, and HEK-293 cell lines were obtained from the National Centre for Cell Science (Pune, India), and maintained as per instructions. The cytotoxicity of the synthesized AgNPs was evaluated by 3-(4, 5-dimethylthiazol-2-yl)-2, 5-diphenyl-tetrazolium bromide (MTT) assay described before [27].

AO/PI staining

HeLa cells were seeded plated in a six well animal cell culture plate and incubated overnight. Next day, cells were treated with different concentrations of the AgNPs after 4 h of serum starvation, and incubated for 24 h. After the incubation, the cells were washed after the incubation with phosphate buffered saline (PBS), and stained with acridine orange (AO)/ propidium iodide (PI) (1:1, 20 µM) [33]. After 30 min of incubation at dark, the cells were observed under microscope, photographs were taken, and analyzed by ImageJ v 1.53a

software.

Hemolysis activity

Hemolysis activity of the silver nanoparticle was evaluated as follows [34]. Two percent of human erythrocyte (RBC) in PBS, pH 7.2 were treated with different concentrations of AgNPs, and incubated at 37 °C for 24 h. TritonX 100 (5%) used as positive control, and PBS used as solvent control. After incubation, the reaction mixtures were centrifuged to separate unlysed cells from supernatant, and measured absorbance at 490 nm against PBS as blank.

$$\text{The \% of RBC lysis} = (A - A_0)/(A_1 - A_0) \times 100$$

Where A is the absorbance of the test samples, A_0 is the absorbance of the solvent control, A_1 is the absorbance of positive control.

Photocatalytic activity

Photocatalytic activity of the synthesized nanoparticles was evaluated using methylene blue (MB) as described previously [35]. Briefly, 10 µg mL^{-1} solutions of the MB were prepared. The AgNPs (200 µg mL^{-1}) was added to the solution, and continued the reaction in presence of light with constant stirring. Periodically, the solutions were scanned using UV-Vis spectrophotometer (Eppendorf BioSpectrometer). The concentration of dye is directly proportional to the absorbance in the UV-Vis spectrophotometer [36]. The percentage of dye degradation, and reaction kinetics were calculated as described earlier [35].

Statistical analysis

All the experiments of the present study were performed in triplet/ or more as mentioned, and the data of the experiments were expressed as mean ± standard deviation (SD). Variance <5% (i.e. $P<0.05$) is considered as a positive result.

RESULTS AND DISCUSSION

C. buchanani leaves are enriched with phytochemicals. During the preparation of nanoparticles, these compounds act as capping and reducing agents [26]. Free electrons present in metal nanoparticles yielding a surface plasmon resonance (SPR) absorption band [29]. Silver nanoparticles exhibit a sharp band around 420 - 440 nm [37]. Fig. 1(A) shows a band at 432 nm, which confirmed the presence of silver nanoparticles in solution.

The TEM result confirms the synthesized silver nanoparticles are round shaped, and around 17.05±5.27 nm in size (Fig. 2(A)). More than 90% particles are distributed between 10-25 nm size. The result is similar to the DLS result (Fig. 4(A)). The nanoparticles are small in size which make it chemically active [38-40].

The functional groups that are present in plant extract acted as reducing agents for the reduction of Ag^{+}ion. In this FTIR spectrum, major peaks were

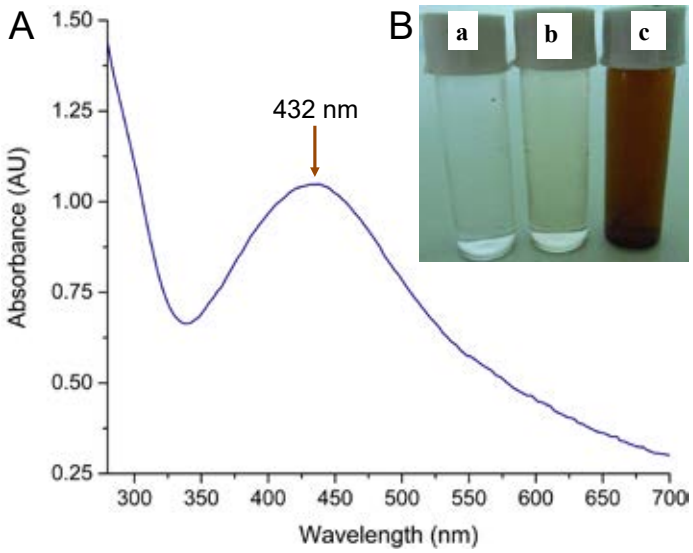

Fig. 1. A) UV-vis spectrum of synthesized nanoparticle showed sharp band at 432 nm, which is characteristic of silver nanoparticles. B) Silver nitrate solution (a), plant extract (b), and colloidal solution after synthesis of nanoparticles (c).

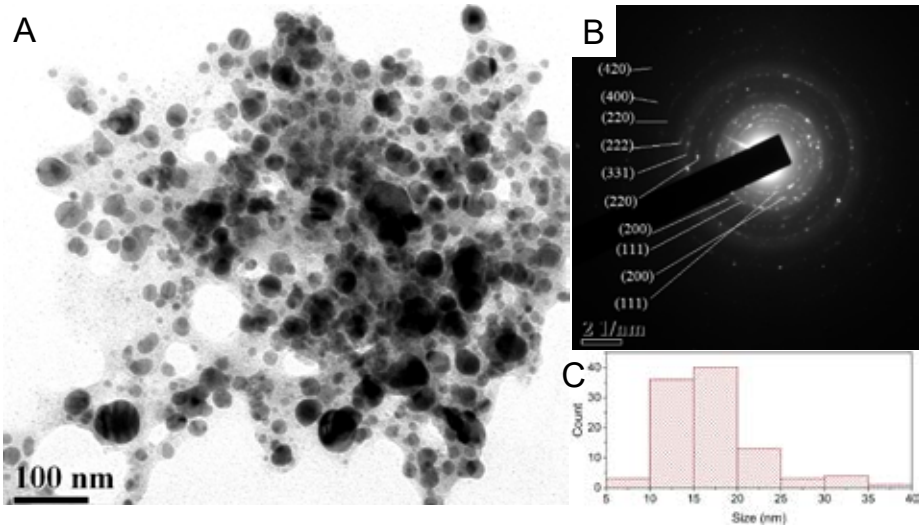

Fig. 2. A) Synthesized nanoparticles's TEM image, scale bar 100 nm. B) Selected area of electron diffraction pattern, C) Particle size distribution.

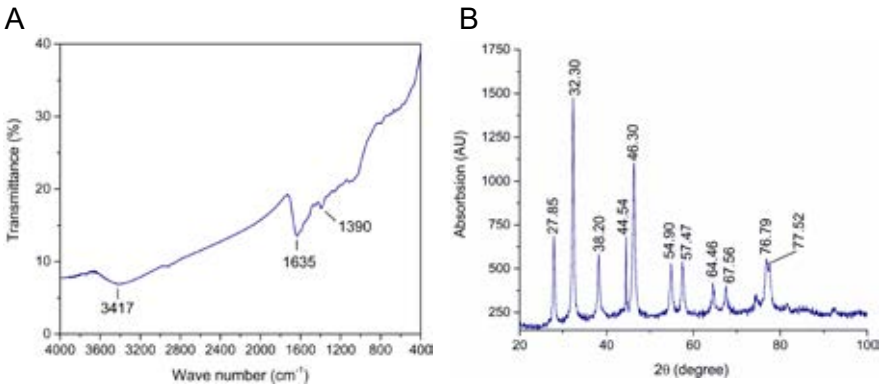

Fig. 3. A) FTIR spectrum, and B) XRD spectrum of the synthesized nanoparticles.

observed at 3417, 1635, 1393 cm^{-1}[Fig. 3(A)]. The broad peak shown at 3417 cm^{-1} was denoted the O-H bond stretch or H bonding. The peak at 1635 $cm^{-1}$was assigned for the N-H bending of amine, and the peak at 1393 cm^{-1}indicated the presence of the phenol groups. Other minor peaks below 1300 cm^{-1} might be due to the various organic groups present in plant extract [41].

X-ray powder diffraction (XRD) analysis confirms the crystalline nature of the synthesized AgNPs was confirmed by. The distinct diffraction peaks at 2θ values of 38.02, 44.54, 64.46 and 77.52 could be indexed to the (111), (200), (220) and (311) reflection planes of face centered cubic structure of silver (Fig. 3(B)). The small peaks might be caused by impurities present in biological extract. Early reports also demonstrated the same type of peaks during the synthesis of silver nanoparticles [42-43]. The 10 sharp peaks shown at 2θ = 27.85, 32.3, 46.3, 54.9, 57.47, 67.56, and 77.52 can be indexed to 111, 200, 220, 311, 222, 400 and 420 planes of the cubic AgCl-NPs (ICDD file no 00-001-1013). The peaks at 38.2, 44.54 and 64.46 are corresponds to the planes of 111, 200, 220 which represent small amount of cubic Ag (ICDD file number 00-087-0718) (Fig 2B). This data also indicates that the synthesis of AgNP is a result of the reduction of Ag^{+} by the presence of the organic compounds in the plant extract.

The short- and long-term stability of emulsions relates to the value of the zeta potential. Emulsions with high negative/positive zeta potential are electrically stable, while emulsions with low zeta potentials tends to coagulate or flocculate [44].

Synthesized AgNPs have a high zeta value of 65 ± 5 mV, and are highly stable in emulsion (Fig 4(B)). In summary the synthesized nanoparticles are round shaped, having an average size of 17.05±5.27 nm, crystalline in nature with a positive surface charge.

Biological activity of the synthesized nanoparticles

Cells from HeLa, MCF-7, and HEK-293 cell lines were treated with different concentrations (0-25 µg mL^{-1}) of the synthesized nanoparticles in-vitro. Results showed that the nanoparticles were specifically more toxic to the HeLa cells. At highest concentration (25 µg mL^{-1}), more than 70 % of the MCF-7 population survived, indicating the nanoparticles have very less toxicity against MCF-7 (Fig. 5 (A)), and not considered for further study. In case of HeLa cells, the nanoparticles killed 26.6, 32.8, 52.0, 82.5, and 91.0 % of the population at 1, 2.5, 5, 10, and 25 µg mL^{-1} concentration respectively (Fig. 5 (A)). The LD_{50} value in our study found 3.98 µg mL^{-1} for HeLa cells. In contrast, the nanoparticles killed 0, 17.5, 35.7, 44.7, 77.9 % of HEK-293 populations, which is a non-cancer cell line, at 1, 2.5, 5, 10, and 25 µg mL^{-1} concentration of the nanoparticles respectively (Fig. 5 (A)), with a 9.45 µg mL^{-1} of LD_{50} value. The LD_{50} value is almost three times higher than the LD50 value found in HeLa, making it unique for its potential application. The nanoparticles lysed less than 2.5 % of human red blood cells at 24 h at 10 µg mL^{-1} (Fig 5. (B)), at the same conditions only ~18% HeLa cells survived.

As the nanoparticles specifically showed better toxicity to the HeLa cells, the nuclear morphology was further studied by propidium iodide (PI), and AO double staining method. The HeLa cells were treated with 1, 5, and 25 µg mL^{-1} of the AgNPs for 24 h, and stained with acridine orange (AO) and propidium iodide (PI) nuclear staining dyes. AO is green fluorescent dye, and permeable to both live and dead cells membrane. PI, which generates red fluorescence, is permeable to dead, and dying apoptotic and necrotic cells membrane. The untreated cells have intact morphology and highly organized nuclei fluorescing green

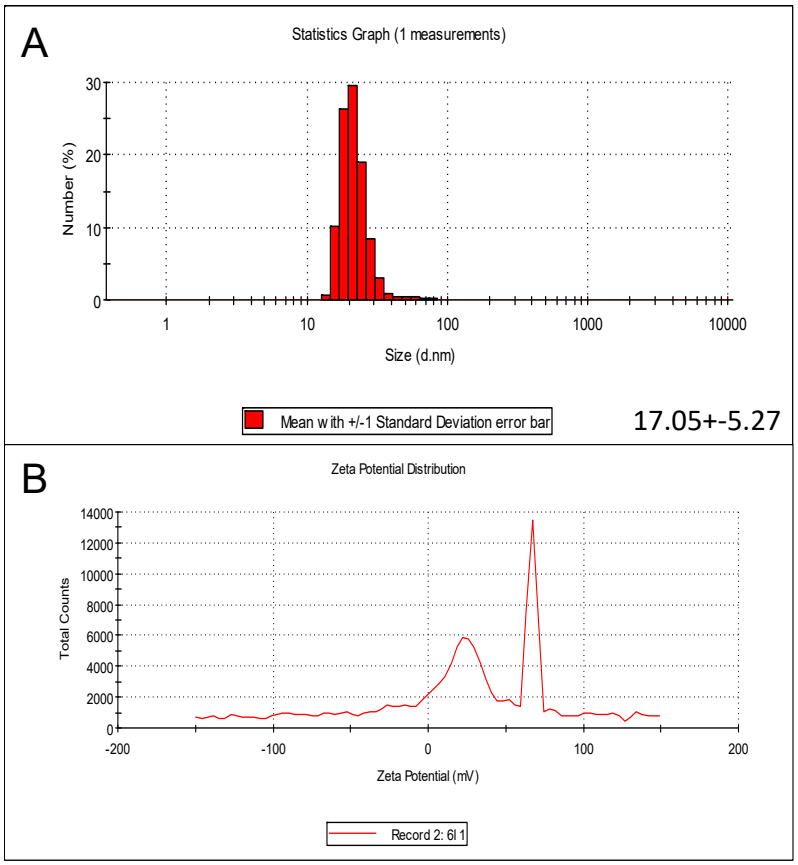

Fig. 4. A) DLS analysis of synthesized nanoparticles. B) Positive Zeta potential indicating the AgNPs have positive surface charge.

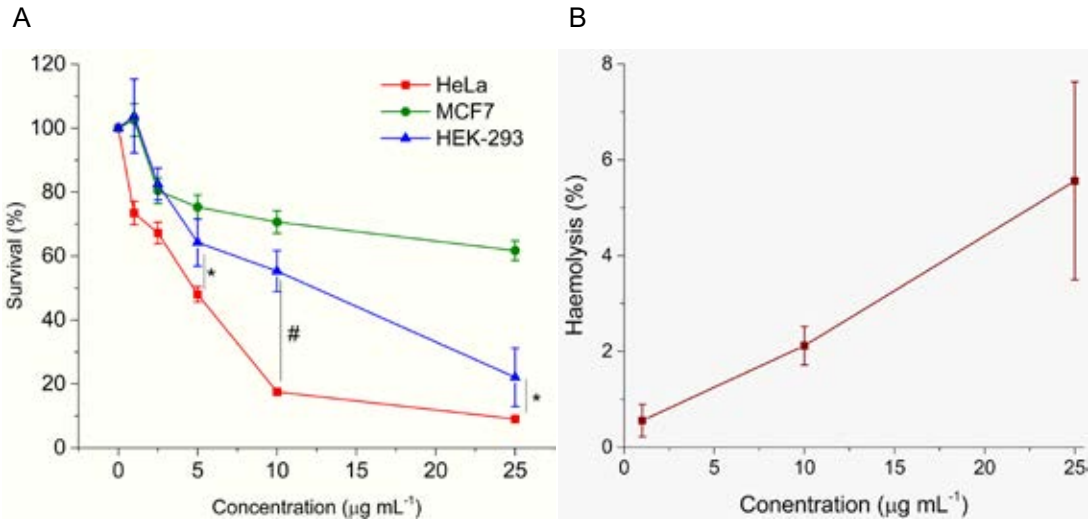

Fig. 5. A) Cytotoxicity of the synthesized nanoparticles against different cell lines at 24 h. Error bar indicating standard deviations (n=6). *, P < 0.5, and #, P <0.001 B) Haemolytic activity of the synthesized nanoparticles at 24 h. n=3, error bar indicating standard deviations.

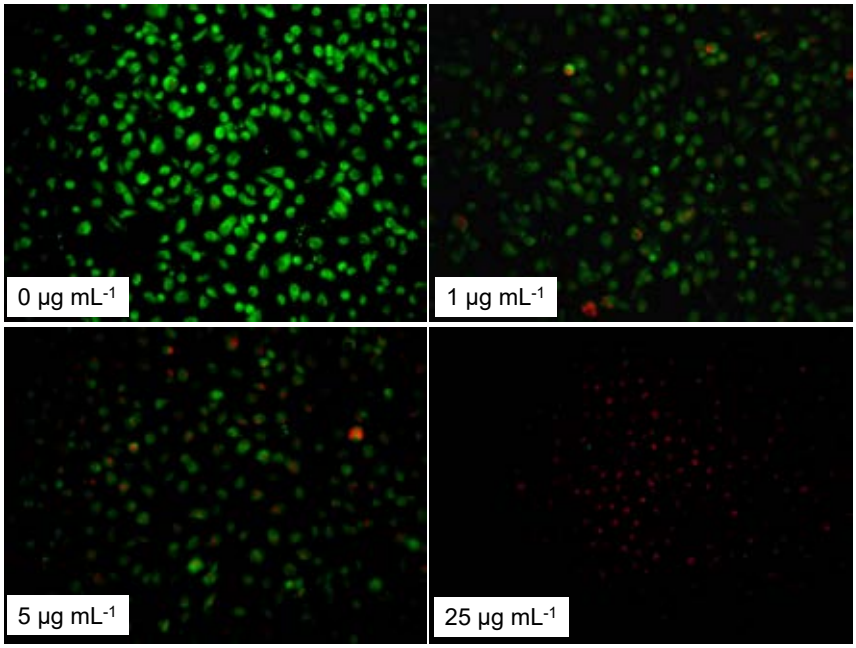

Fig. 6. AO/PI staining after treatment with different concentration of the AgNPs for 24 h.

color (Fig. 6) as PI not permeable to live cell membrane. Cells with increasing concentration of the AgNPs showed morphological the changes in the cell nuclei morphology change which relate to apoptosis fluorescing orange to red. In lower concentrations of the nanoparticles, fewer cells fluoresce orange indicating early apoptosis. At highest concentration almost all nuclei fluoresce red which is the indication of late apoptosis (Fig. 6) [45,46]. Decreasing of cell number is observed in case of treated cells as compared to control, which is proportional to the concentration of the AgNPs, also validates MTT assay results. The above results showed that the synthesized AgNPs have promising characteristics and might be studied further for its potential application in the field of cancer biology.

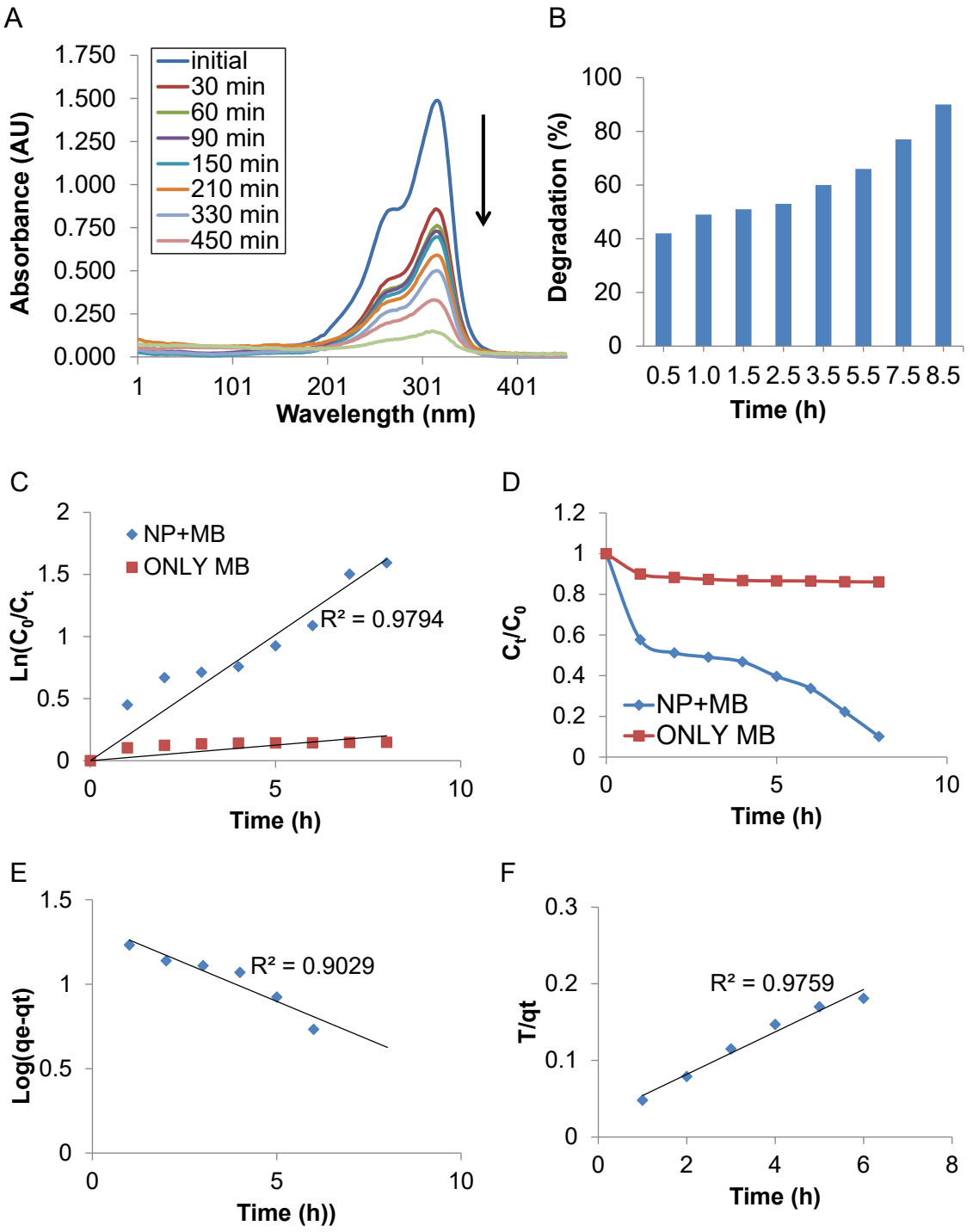

Fig. 7. A) UV spectra showed methylene blue (MB) degradation activity of the synthesized AgNPs in presence of light B) Represent the % of MB degration over time C) Kinetic fit plot of ln (C_0/C_t) vs time in case of methylene blue (MB) and nanoparticles (NPs) in presence of light. Here C_0 was initial dye concentration and C_t was the concentration of dye at time t. D) Degradation of only methylene blue (MB) and methylene blue in presence of nanoparticles (NP + MB) E) Pseudo first order models of photocatalytic activity F) Pseudo second order models of photocatalytic activity.

Photocatalytic activity

In the presence of light, we study the photo catalytic activity of the AgNP using methylene blue. The concentration of the dye in this solution is equal to the absorbance of the solution at 660 nm. The result showed increasing the exposure time of the solution of dye and AgNP in presence of light, the pick is decreasing due to the degradation of dye (Fig. 7(A)). The AgNP degraded 49% dye in 1 h exposure, and 60% dye in 3.5 h exposure. After 8.5 h of incubation, more than 90% dye was degraded (Fig. 7(B)). The presence of the nanoparticles along with light, accelerated degradation rate of the methylene blue, in comparison when only light is present (Fig. 7 (D)). (Fig X (E)) represents the pseudo 1st order reaction model, which is not a good fit due to low correlation coefficient value (R^2 = 0.9029). A liner plot was observed when t/qt was plotted against time. Higher value of correlation coefficient (R^2 = 0.9759), which is closed to 1, indicating the reaction followed pseudo 2nd order kinetic (Fig. 7(E)) [35].

CONCLUSION

In conclusion, this is the first study that attempted to synthesize silver nanoparticles from *C. buchanani* plant material, which is enriched with different phytochemicals. The small size of the synthesized nanoparticles makes it chemically active. The nanoparticles showed two distinct properties, it killed specifically HeLa cells *in vitro*, probably by inducing apoptosis. It is also capable of degrading more than 90 % of methylene blue in presence of light at 8.5 h. Both characteristics make the nanoparticles promising for future study.

ACKNOWLEDGEMENT

Author is grateful to DBT-BOOST (Govt. of West Bengal) and DST-FIST (Govt. of India) for instrumentation support.

CONFLICT OF INTEREST

The authors declare that no competing interest exists.

CONTRIBUTION

SP- Experimental sections, AP- Hemolysis, AO/PI staining, KK- Conceptualization, Cytotoxicity study, IC- Manuscript preparation, BP- Conceptualization, NB- Conceptualization, supervise, preparation of final manuscript.

REFERENCES

1. Endress ME, Bruyns PV. A revised classification of the Apocynaceae s.l. The Botanical Review. 2000;66(1):1-56.
2. Sanyal N. Agro-techniques of Selected Medicinal Plants. 2014; Vol II: pp 34-36.
3. Bhakuni DS, Dhar ML, Dhar MM, Dhawan BN, Mehrotra BN. Screening of Indian plants for biological activity, 1969; II: 250-262.
4. Tayung K and Saikia N. 2003. Cryptolepis buchanani—A less-known medicinal plant used in bone fracture. Indian Jurnal of traditional knowledge, 2003;2(4): 371-374.
5. Kaul A, Bani S, Zutshi U, Suri KA, Satti NK, Suri OP. Immunopotentiating properties ofCryptolepis buchanani root extract. Phytotherapy Research. 2003;17(10):1140-4.
6. Sunil K, Batuk D, Sharma N, Sharria PV. A new nicotinoyl glucoside from Cryptolepis buchanani. Phytochemistry. 1980;19(6):1278.
7. Khare MP, Shah BB. Structure of buchanin, a new cardenolide from Cryptolepis buchanani Roem. &Schult. Journal of Nepal Chemical Society. 1983;3:21-30.
8. Purushothaman KK, Vasanth S, Connolly JD, Rycroft DS. New sarverogenin and isosarverogenin glycosides from Cryptolepis buchanani (Asclepiadaceae). RevistaLatinoamericana de Quimica. 1988;19(1):28-31.
9. Venkateswara R, Narendra N, Viswamitra MA, Vaidyanathan CS. Cryptosin, a cardenolide from the leaves of Cryptolepis buchanani. Phytochemistry. 1989;28(4):1203-5.
10. Pande M, Dubey VK, Yadav SC, Jagannadham MV. A Novel Serine Protease Cryptolepain fromCryptolepis buchanani: Purification and Biochemical Characterization. Journal of Agricultural and Food Chemistry. 2006;54(26):10141-50.
11. Laupattarakasem P, Wangsrimongkol T, Surarit R, Hahnvajanawong C. In vitro and in vivo anti-inflammatory potential of Cryptolepis buchanani. Journal of Ethnopharmacology. 2006;108(3):349-54.
12. Hanprasertpong N, Teekachunhatean S, Chaiwongsa R, Ongchai S, Kunanusorn P, Sangdee C, et al. Analgesic, Anti-Inflammatory, and Chondroprotective Activities ofCryptolepis buchananiExtract:In VitroandIn VivoStudies. BioMed Research International. 2014;2014:1-8.
13. Padmalochana K. Evaluation of the Antioxidant and Hepatoprotective Activity of Cryptolepis Buchanani. Journal of Applied Pharmaceutical Science. 2013.
14. Ashwini SK, Kiran R, Soumya KV, Sudharshan SJ, PrashithKekuda TR, Vinayaka KS, Raghavendra HL. Insecticidal and in vitro antioxidant potency of extracts of Cryptolepis buchanani Roem. &Schult. Int J Ph Sci. 2010 Jan; 2(1):418-25.
15. Vinayaka KS, Prashith KTR, Mallikarjun N, Sateesh VN. Anti-dermatophyte activity of Cryptolepis buchanani Roem. & Schult. Pharmacognosy Journal. 2010;2(7):170-2.
16. Wongyai K, Wintachai P, Maungchang R, Rattanakit P. Exploration of the Antimicrobial and Catalytic Properties of Gold Nanoparticles Greenly Synthesized by Cryptolepis buchanani Roem. and Schult Extract. Journal of Nanomaterials. 2020;2020:1-11.
17. Karthiga Devi G, Senthil Kumar P, Sathish Kumar K. Green synthesis of novel silver nanocomposite hydrogel based on sodium alginate as an efficient biosorbent for the dye wastewater treatment: prediction of isotherm and kinetic parameters. Desalination and Water Treatment. 2016:1-14.
18. Awwad AM. Phytochemical Fabrication And Character-

ization Of Silver/ Silver Chloride Nanoparticles Using Albizia Julibrissin Flowers Extract. Advanced Materials Letters. 2015;6(8):726-30.
19. Yugandhar P, Savithramma N. Leaf Assisted Green Synthesis of Silver Nanoparticles from Syzygium Alternifolium (Wt.) Walp. Characterization and Antimicrobial Studies. Nano Biomedicine and Engineering. 2015;7(2).
20. Marutikesavakumar C, Yugandhar P, Savithramma N. Adansonia digitata leaf extract mediated synthesis of silver nanoparticles; characterization and antimicrobial studies. Journal of Applied Pharmaceutical Science. 2015:082-9.
21. Gnanajobitha G, Paulkumar K, Vanaja M, Rajeshkumar S, Malarkodi C, Annadurai G, et al. Fruit-mediated synthesis of silver nanoparticles using Vitis vinifera and evaluation of their antimicrobial efficacy. Journal of Nanostructure in Chemistry. 2013;3(1).
22. Omobayo Adio S, Basheer C, Zafarullah K, Alsharaa A, Siddiqui Z. Biogenic synthesis of silver nanoparticles; study of the effect of physicochemical parameters and application as nanosensor in the colorimetric detection of Hg2+ in water. International Journal of Environmental Analytical Chemistry. 2016;96(8):776-88.
23. Ahmed S, Ahmad M, Swami BL, Ikram S. A review on plants extract mediated synthesis of silver nanoparticles for antimicrobial applications: A green expertise. Journal of Advanced Research. 2016;7(1):17-28.
24. Sharma VK, Yngard RA, Lin Y. Silver nanoparticles: Green synthesis and their antimicrobial activities. Advances in Colloid and Interface Science. 2009;145(1-2):83-96.
25. Nair R, Varghese SH, Nair BG, Maekawa T, Yoshida Y, Kumar DS. Nanoparticulate material delivery to plants. Plant Science. 2010;179(3):154-63.
26. Panja S, Chaudhuri I, Khanra K, Bhattacharyya N. Biological application of green silver nanoparticle synthesized from leaf extract of Rauvolfia serpentina Benth. Asian Pacific Journal of Tropical Disease. 2016;6(7):549-56.
27. Khanra K, Panja S, Choudhuri I, Chakraborty A, Bhattacharyya N. Evaluation of Antibacterial Activity and Cytotoxicity of Green Synthesized Silver Nanoparticles Using Scoparia Dulcis. Nano Biomedicine and Engineering. 2015;7(3).
28. Khanra K, Panja S, Choudhuri I, Chakraborty A, Bhattacharyya N. Bactericidal and Cytotoxic Properties of Silver Nanoparticle Synthesized from Root Extract of Asparagus Racemosus. Nano Biomedicine and Engineering. 2016;8(1).
29. Ibrahim HMM. Green synthesis and characterization of silver nanoparticles using banana peel extract and their antimicrobial activity against representative microorganisms. Journal of Radiation Research and Applied Sciences. 2015;8(3):265-75.
30. Singh K, Panghal M, Kadyan S, Chaudhary U, Yadav JP. Green silver nanoparticles of Phyllanthus amarus: as an antibacterial agent against multi drug resistant clinical isolates of Pseudomonas aeruginosa. Journal of Nanobiotechnology. 2014;12(1).
31. Anandalakshmi K, Venugobal J, Ramasamy V. Characterization of silver nanoparticles by green synthesis method using Pedalium murex leaf extract and their antibacterial activity. Applied Nanoscience. 2015;6(3):399-408.
32. Reena K, Balashanmugam P, Gajendiran M, Antony SA. Synthesis of *Leucas Aspera* Extract Loaded Gold-PLA-PEG-PLA Amphiphilic Copolymer Nanoconjugates: *In Vitro* Cytotoxicity and Anti-Inflammatory Activity Studies. Journal of Nanoscience and Nanotechnology. 2016;16(5):4762-70.
33. Parsekar SU, Velankanni P, Sridhar S, Haldar P, Mate NA, Banerjee A, et al. Protein binding studies with human serum albumin, molecular docking and in vitro cytotoxicity studies using HeLa cervical carcinoma cells of Cu(ii)/Zn(ii) complexes containing a carbohydrazone ligand. Dalton Transactions. 2020;49(9):2947-65.
34. Dobrovolskaia MA, Clogston JD, Neun BW, Hall JB, Patri AK, McNeil SE. Method for Analysis of Nanoparticle Hemolytic Properties in Vitro. Nano Letters. 2008;8(8):2180-7.
35. Panja S, Choudhuri I, Khanra K, Pati B, Bhattacharyya N. Biological and Photocatalytic Activity of Silver Nanoparticle Synthesized from Ehretia laevis Roxb. Leaves Extract. Nano Biomedicine and Engineering. 2020;12(1).
36. Roy K, Sarkar CK, Ghosh CK. Photocatalytic activity of biogenic silver nanoparticles synthesized using yeast (Saccharomyces cerevisiae) extract. Applied Nanoscience. 2014;5(8):953-9.
37. Mulvaney P. Surface Plasmon Spectroscopy of Nanosized Metal Particles. Langmuir. 1996;12(3):788-800.
38. Akbari B, Tavandashti MP, Zandrahimi M. Particle size characterization of nanoparticles–a practicalapproach. Iranian Journal of Materials Science and Engineering. 2011 Jun 10;8(2):48-56.
39. Baer DR. Surface Characterization of Nanoparticles: *critical needs and significant challenges*. JSA. 2011;17(3):163–9.
40. Yacaman MJ, Ascencio JA, Liu HB. Gardea (Torresdey, J. Journal of Vacuum Science and Technology, B: Microelectronics and Nanometer Structures. 2001; 19:1091-103.
41. Griffiths PR, de Haseth JA. Fourier Transform Infrared Spectrometry: John Wiley & Sons, Inc.; 2007 2007/04/20.
42. Paulkumar K, Gnanajobitha G, Vanaja M, Rajeshkumar S, Malarkodi C, Pandian K, et al. Piper nigrumLeaf and Stem Assisted Green Synthesis of Silver Nanoparticles and Evaluation of Its Antibacterial Activity Against Agricultural Plant Pathogens. The Scientific World Journal. 2014;2014:1-9.
43. Arockia John Paul J, Karunai Selvi B, Karmegam N. Biosynthesis of silver nanoparticles from Premna serratifolia L. leaf and its anticancer activity in CCl4-induced hepato-cancerous Swiss albino mice. Applied Nanoscience. 2015;5(8):937-44.
44. Lu GW, Gao P. Emulsions and Microemulsions for Topical and Transdermal Drug Delivery. Handbook of Non-Invasive Drug Delivery Systems: Elsevier; 2010. p. 59-94.
45. Koley MK, Duraipandy N, Kiran MS, Varghese B, Manoharan PT, Koley AP. DNA binding and cytotoxicity of some Cu(II)/Zn(II) complexes containing a carbohydrazone Schiff base ligand along with 1,10-phenanthroline as a coligand. Inorganica Chimica Acta. 2017;466:538-50.
46. Koley MK, Parsekar SU, Duraipandy N, Kiran MS, Varghese B, Manoharan PT, et al. DNA binding and cytotoxicity of two Cu(II) complexes containing a Schiff base ligand along with 1,10-phenanthroline or imidazole as a coligand. Inorganica Chimica Acta. 2018;478:211-21.